



LABORATOIRE
JEAN KUNTZMANN
MATHÉMATIQUES APPLIQUÉES • INFORMATIQUE



On the discretization of vertical diffusion in the turbulent surface and planetary boundary layers

F. Lemarié – Inria (EPC AIRSEA), Laboratoire Jean Kuntzmann, Grenoble, France

In collaboration with: E. Blayo & S. Théry (UGA), C. Pelletier (UCLouvain), F. Nazari (Inria)

Context: representation of mixing in PBLs

▷ Reynolds averaging ($\phi = \langle \phi \rangle + \phi'$)

$$\partial_t \langle \phi \rangle = \dots + \text{div}(\langle \mathbf{u}' \phi' \rangle) + \dots$$

▷ Diffusive approach for "local" mixing (K-theory)

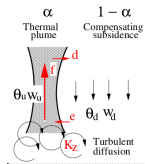
⇒ Boundary layer approximations: horiz. homogeneity and eddy diffusion

$$\langle w' \phi' \rangle = -K \partial_z \langle \phi \rangle \quad \rightarrow \quad \partial_t \langle \phi \rangle = \dots + \partial_z (K \partial_z \langle \phi \rangle) + \dots$$

→ Down-gradient fluxes

→ Turbulence acts as a "mixing"

▷ Mass flux approach for "non-local" mixing (e.g. Chatfield & Brost, 1987; Siebesma, 2007)



$$\langle w' \phi' \rangle = -K \partial_z \langle \phi \rangle + \alpha w_u (\phi_u - \langle \phi \rangle) \quad \rightarrow \quad \partial_t \langle \phi \rangle = \partial_z (K \partial_z \langle \phi \rangle) - \partial_z (\alpha w_u \langle \phi \rangle) + \dots$$

⇒ advection-diffusion operator to parametrize unresolved scales in PBLs and beyond (e.g. internal wave breaking or convective adjustment)

Context: representation of mixing in PBLs

Standard schemes to provide K :

- 0-equation: algebraic computation of the eddy parameters from bulk properties
- 1-equation: prog. eqn for turbulent kinetic energy (TKE) + diagnostic mixing length
- 2-equations: prog. eqn for TKE and for a "generic" length scale (ϵ , ω , ...)

The resulting turbulent viscosity/diffusivity K

- strongly varies spatially (internal & boundary layers), i.e. large values of $\frac{h(\partial_z K)}{K}$
- depends nonlinearly on model variables
- induces stiffness i.e. large vertical parabolic Courant numbers $\sigma^{(2)} = \frac{K \Delta t}{h^2}$

Usual approach (e.g. WRF, LMDZ, all oceanic models):

use of (semi)-implicit temporal schemes with 2nd-order FD discretization

Context: standard approach

- **What could be wrong with second-order scheme in space ?**

- Nothing . . . if pure diffusion (i.e. with constant K) is considered

$$\partial_z (K \partial_z \phi)_k^{(C2)} = \partial_z (K \partial_z \phi)_k + \frac{h^2}{12} \left\{ K \partial_z^4 \phi \right\} + \mathcal{O}(\Delta z^4)$$

- but with $\text{Pe}^{(n)} = \frac{h^n \partial_z^n K}{K} \neq 0, n \geq 1$

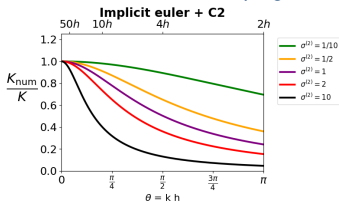
$$\partial_z (K \partial_z \phi)_k^{(C2)} = \partial_z (K \partial_z \phi)_k + \frac{1}{24} \partial_z \left(K \left[\text{Pe}^{(2)} \partial_z \phi + 2 \Delta z \text{Pe}^{(1)} \partial_z^2 \phi + 2 \Delta z^2 \partial_z^3 \phi \right] \right) + \mathcal{O}(\Delta z^4)$$

- **What could be wrong with (semi)-implicit scheme in time ?**

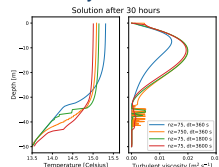
- Lack of monotonic damping (e.g. **Manfredi & Ottaviani, 1999; Wood et al., 2007**)
possibly leaving noise uncontrolled (+ trigger conv. adjust.)
- Inexact damping for large $\sigma^{(2)}$
- $\mathcal{O}(\Delta t)$ errors in coupling with physical parameterizations

Impact on model solutions

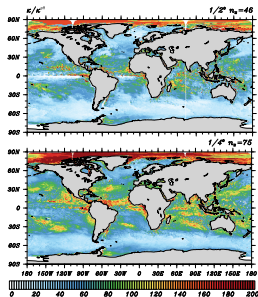
numerical vs exact damping rate



Sensitivity to Δt and Δz



Single-column exp. (Wind-induced deepening of BL)



Maps of K/K^{num} from oceanic realistic simulations

- K^{num} is the diffusivity in the continuous equation with same damping as the numerical damping
- $K/K^{\text{num}} \gg 1 \Rightarrow$ the damping seen by the model is smaller than the theoretical damping.
- $\sigma^{(2)} = \overline{\sigma^{\text{mld}}}, \theta = \frac{2\pi}{N_{\text{mld}}}.$

Objectives

- ▷ Have a better control of numerical sources of error independently from the physical principles of the subgrid scheme
- ▷ Consistency between the parameterizations and the resolved fluid dynamics (for bottom boundary condition & $K(z)$ computation)

Outline

1. Spatial discretization
2. Treatment of the bottom boundary condition (MO consistency)
3. Combination with time discretization
4. Combination with subgrid closure schemes

1

Spatial discretization

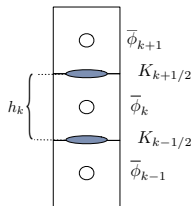
Objectives & motivations

Constraints

- limit ourselves to tridiagonal linear problems
- possibility to have a joint treatment of vertical advection and diffusion
- allow a finite-volume interpretation

Possible alternatives

- ▷ Exponential Compact scheme
(e.g. McKinnon & Johnson, 1991; Tian & Dai, 2007)
→ Specifically designed for accuracy with large Peclet numbers
- ▷ Padé compact finite volume discretization



General form of the discretization

$$\partial_z(K\partial_z\phi) = \frac{K_{k+1/2}d_{k+1/2} - K_{k-1/2}d_{k-1/2}}{h_k}, \quad d_{k+1/2} = (\partial_z\phi)_{k+1/2}$$

for standard discretization: $d_{k+1/2} = (\phi_{k+1} - \phi_k)/h$ (h : vertical layers thickness)

Parabolic splines reconstruction

Suppose a given set of $\{\bar{\phi}_k, k = 1, \dots, N\}$ and assume a subgrid parabolic reconstruction

$$\phi(\xi) = a\xi^2 + b\xi + c, \quad \xi \in \left[-\frac{h_k}{2}, \frac{h_k}{2}\right]$$

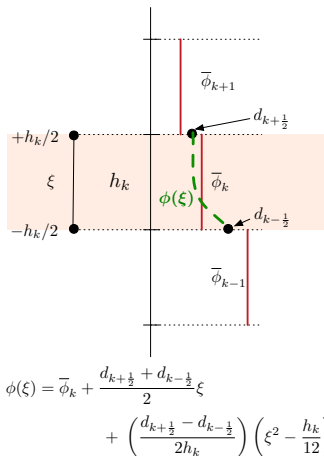
under the constraints

- $\frac{1}{h_k} \int_{-\frac{h_k}{2}}^{\frac{h_k}{2}} \phi(\xi) d\xi = \bar{\phi}_k$
- $\partial_z \phi(+h_k/2) = d_{k+1/2}, \partial_z \phi(-h_k/2) = d_{k-1/2}$

+ Impose the continuity of ϕ at cell interfaces :

$$\frac{1}{6} \mathbf{d}_{k+3/2} + \frac{2}{3} \mathbf{d}_{k+1/2} + \frac{1}{6} \mathbf{d}_{k-1/2} = \frac{\bar{\phi}_{k+1} - \bar{\phi}_k}{h}$$

- necessitates inversion of an implicit linear system of equations
- *compact* accuracy (4th-order for advection, 2nd for diffusion)
- Widely used for vertical advection in oceanic models



Compact Padé Finite Volume methods

Lele, 1992; Kobayashi, 1999

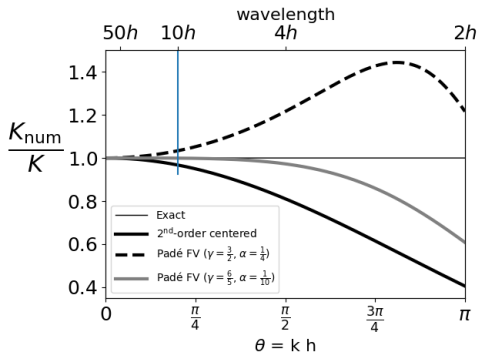
Unknowns : derivatives $d_{k+\frac{1}{2}}$ on cell interfaces, for $m, n \in \mathcal{N}$

$$\sum_{i=1}^m \alpha_i d_{k+\frac{1}{2}-i} + d_{k+\frac{1}{2}} + \sum_{i=1}^m \alpha_i d_{k+\frac{1}{2}+i} = \frac{1}{h} \left(\sum_{j=1}^n \gamma_j \bar{\phi}_{k+j} - \sum_{j=1}^n \gamma_j \bar{\phi}_{k-j+1} \right)$$

- For $(m, n) = (1, 1)$: $\alpha_1 d_{k-\frac{1}{2}} + d_{k+\frac{1}{2}} + \alpha_1 d_{k+\frac{3}{2}} = \gamma_1 \left(\frac{\bar{\phi}_{k+1} - \bar{\phi}_k}{h} \right)$
 $(\alpha_1, \gamma_1) = \left(\frac{1}{10}, \frac{6}{5} \right) \rightarrow$ 4th-order discretization of $d_{k+\frac{1}{2}}$ (for $K = \text{cste}$)
 $(\alpha_1, \gamma_1) = \left(\frac{1}{4}, \frac{3}{2} \right) \rightarrow$ equivalent to parabolic splines reconstruction.

- Can be reinterpreted in terms of subgrid reconstruction as parabolic splines
- Flexibility provided by α and γ parameters

Effective viscosity/diffusivity



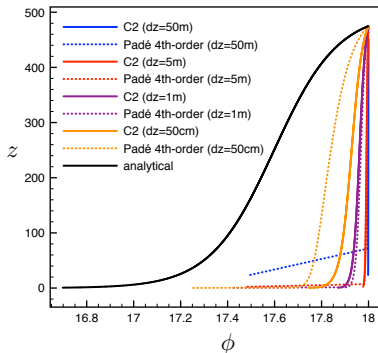
- At this point relevant only for internal layers
→ not directly applicable to turbulent boundary layers
- Illustration : stationary problem

$$\left\{ \begin{array}{lcl} \partial_z (K(z) \partial_z \phi) & = & \frac{\partial_z \mathcal{R}}{\rho C_p} \\ \phi(0) & = & \phi_{\text{bot}} \\ \phi\left(\frac{19h_{\text{bl}}}{20}\right) & = & \phi_{\text{top}} \end{array} \right.$$

with

$$K(z) = \kappa \phi_{\star} \frac{z}{h_{\text{bl}}} (h_{\text{bl}} - z) + K_{\text{mol}}$$

$$\mathcal{R}(z) = \mathcal{R}_0 \left(\alpha e^{-z/\zeta_0} + (1 - \alpha) e^{-z/\zeta_1} \right)$$



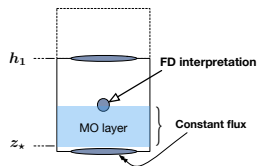
2

Treatment of the bottom boundary condition (MO consistency)

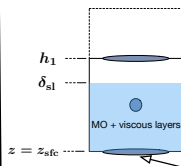
Treatment of boundary cells (neutral case)

Dirichlet boundary condition is never applied in practice

→ replaced by a flux condition consistent with wall laws

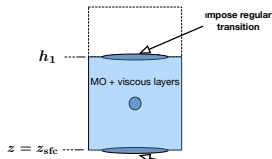


Current practice



Knowledge of local value and gradient

Possible FV alternatives



Knowledge of local value and gradient

Current practice :

$$\begin{cases} \partial_z (\kappa |\phi_*| (z + z_*) \partial_z \phi) = 0 \\ \phi(z_*) = \chi_{\text{sfc}} \\ \phi(h_1/2) = \phi_1 \end{cases}$$

$$\phi(z) = (\phi_1 - \chi_{\text{sfc}}) \left(\frac{\ln \left(\frac{1}{2} + \frac{z}{2z_*} \right)}{\ln \left(\frac{1}{2} + \frac{h_1}{4z_*} \right)} \right) + \chi_{\text{sfc}}$$

FV approach with $h_1 = \delta_{\text{sl}}$:

$$\begin{cases} \partial_z (\kappa |\phi_*| (z + z_*) \partial_z \phi) = 0 \\ \phi(z_{\text{sfc}}) = \chi_{\text{sfc}} \\ \phi(h_1) = \phi_{3/2} \end{cases}$$

$$\phi(z) = (\phi_{3/2} - \chi_{\text{sfc}}) \left(\frac{\ln \left(1 + \frac{z}{z_*} \right)}{\ln \left(1 + \frac{h_1}{z_*} \right)} \right) + \chi_{\text{sfc}}$$

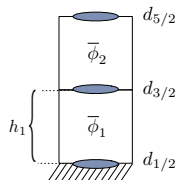
Treatment of boundary cells with Parabolic splines

2nd-order polynomial subgrid reconstruction for $z \in] -\frac{h_k}{2}, \frac{h_k}{2} [$:

$$\phi(z) = \bar{\phi}_k + \left(\frac{d_{k+1/2} + d_{k-1/2}}{2} \right) z + \frac{d_{k+1/2} - d_{k-1/2}}{2h_k} \left(z^2 - \frac{h_k}{12} \right)$$

Usual treatment of boundary cell (with Dirichlet B.C.)

$$\phi\left(-\frac{h_1}{2}\right) = \bar{\phi}_1 - \frac{h_1}{3}d_{1/2} - \frac{h_1}{6}d_{3/2} = \chi_{\text{sfc}} \rightarrow \frac{1}{3}d_{1/2} + \frac{1}{6}d_{3/2} = \frac{\bar{\phi}_1 - \chi_{\text{sfc}}}{h_1}$$



Alternative treatment

$$\phi(z) = (\phi_{3/2} - \chi_{\text{sfc}}) \left(\frac{\ln\left(1 + \frac{z}{z_\star}\right)}{\ln\left(1 + \frac{h_1}{z_\star}\right)} \right) + \chi_{\text{sfc}} = d_{3/2}(h_1 + z^\star) \ln\left(1 + \frac{z}{z_\star}\right) + \chi_{\text{sfc}}$$

$$\rightarrow d_{1/2} = d_{3/2} \left(1 + \frac{h}{z_\star} \right) \quad (\text{consistant with constant flux layer})$$

$$\rightarrow \frac{1}{6}d_{5/2} + \left[\frac{1}{3} + \left(1 + \frac{z_\star}{h} \right) \ln\left(1 + \frac{h}{z_\star} \right) \right] d_{3/2} = \frac{\bar{\phi}_2 - \chi_{\text{sfc}}}{h} \quad (\text{impose regularity})$$

Treatment of boundary cells with Parabolic splines

- **Asymptotics :**

Resolved case (combining the first 2 lines of the matrix)

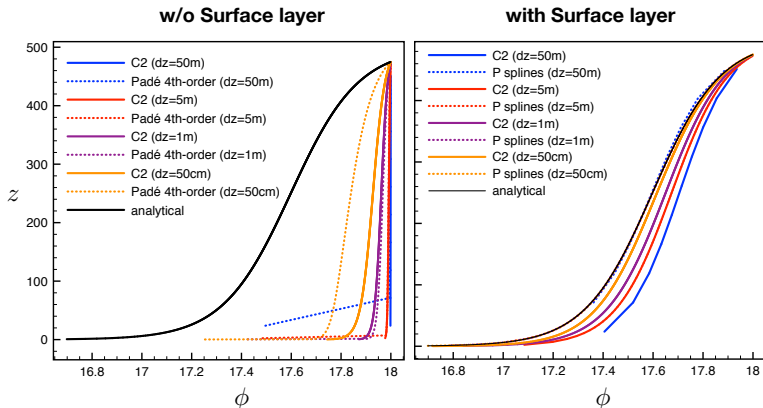
$$\frac{1}{6}d_{5/2} + \frac{5}{6}d_{3/2} + \frac{1}{2}d_{1/2} = \frac{\bar{\phi}_2 - \chi_{\text{sfc}}}{h}$$

Unresolved case (for $h \rightarrow 0$)

$$\frac{1}{6}d_{5/2} + \underbrace{\left(\frac{1}{3} + \left[1 + \frac{h}{2z_*} \right] \right)}_{\frac{5}{6}d_{3/2} + \frac{1}{2}d_{1/2}} d_{3/2} = \frac{\bar{\phi}_2 - \chi_{\text{sfc}}}{h}$$

Smooth transition between the unresolved and the resolved limit.

A numerical example (with $z_\star = K_{\text{mol}}/(\kappa|\phi_\star|)$)



3

Combination with time discretization

Combination with implicit time discretization

Combine Padé-type schemes with implicit Euler :

$$\left\{ \begin{array}{l} \alpha d_{k+3/2}^{n+1} + d_{k+1/2}^{n+1} + \alpha d_{k-1/2}^{n+1} = \gamma \frac{\bar{\phi}_{k+1}^{n+1} - \bar{\phi}_k^{n+1}}{h} \\ \bar{\phi}_k^{n+1} = \bar{\phi}_k^n + \frac{\Delta t}{h} \left[K_{k+1/2} d_{k+1/2}^{n+1} - K_{k-1/2} d_{k-1/2}^{n+1} \right] + \Delta t \text{ rhs}_k \\ \bar{\phi}_{k+1}^{n+1} = \bar{\phi}_{k+1}^n + \frac{\Delta t}{h} \left[K_{k+3/2} d_{k+3/2}^{n+1} - K_{k+1/2} d_{k+1/2}^{n+1} \right] + \Delta t \text{ rhs}_{k+1} \end{array} \right.$$

to end up with the following single tridiagonal problem

$$\begin{aligned} \left(\frac{\alpha}{\gamma} - \frac{K_{k+3/2} \Delta t}{h^2} \right) d_{k+3/2}^{n+1} + \left(\frac{1}{\gamma} + 2 \frac{K_{k+1/2} \Delta t}{h^2} \right) d_{k+1/2}^{n+1} + \left(\frac{\alpha}{\gamma} - \frac{K_{k-1/2} \Delta t}{h^2} \right) d_{k-1/2}^{n+1} \\ = \frac{\bar{\phi}_{k+1}^n - \bar{\phi}_k^n}{h} + \frac{\Delta t}{h} (\text{rhs}_{k+1} - \text{rhs}_k) \end{aligned}$$

- easy to generalize for non-constant grid-size
- The tridiagonal solve provides the flux and not $\bar{\phi}$

Temporal discretization for diffusion

Relevant properties for a well-behaved numerical solution

(e.g. **Manfredi & Ottaviani (1999)**; **Wood et al. (2007)**)

- Unconditional stability
 - Monotonic damping (damping increases with increasing wavenumber, i.e. $\partial_\theta \mathcal{A} < 0$)
 - Non-oscillatory (i.e. $\mathcal{A} \geq 0$)
 - Proper control of grid-scale noise $\forall \sigma^{(2)}$
- Convergence & stability are often not sufficient

Temporal discretization for diffusion

Existing alternatives :

- 1. Crank-Nicolson** : ill-behaved for large time-steps
→ short wave-lengths not damped efficiently
- 2. 2nd-order "Padé" 2-step scheme** (e.g Manfredi & Ottaviani 1999; Wood et al. 2007) :

$$\begin{cases} (1 + a(K\Delta t)\tilde{k}^2)\phi^* &= (1 + b(K\Delta t)\tilde{k}^2)\phi^n \\ (1 + b(K\Delta t)\tilde{k}^2)\phi^{n+1} &= \phi^* \end{cases} \quad \begin{aligned} a &= 1 + \sqrt{2}, \\ b &= 1 + 1/\sqrt{2} \end{aligned}$$

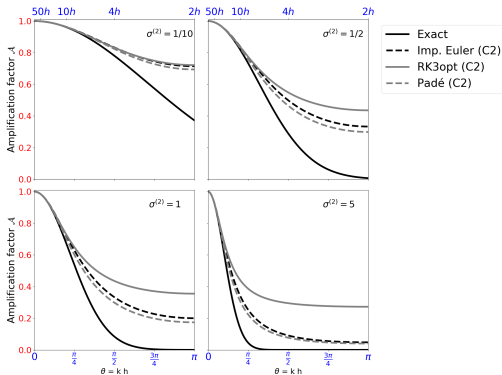
- 3. Diagonally-implicit RK** (e.g Nazari et al., (2013,2014))

$$\begin{cases} \phi^{(1)} &= \phi^n + (K\Delta t)\tilde{k}^2 a_{11}\phi^{(1)} \\ \phi^{(2)} &= \phi^n + (K\Delta t)\tilde{k}^2 (a_{21}\phi^{(1)} + a_{22}\phi^{(2)}) \\ \phi^{(3)} &= \phi^n + (K\Delta t)\tilde{k}^2 (a_{31}\phi^{(1)} + a_{32}\phi^{(2)} + a_{33}\phi^{(3)}) \\ \phi^{n+1} &= \phi^n + (K\Delta t)\tilde{k}^2 (b_1\phi^{(1)} + b_2\phi^{(2)} + b_3\phi^{(3)}) \end{cases}$$

Temporal discretization for diffusion

Existing alternatives :

2. 2nd-order two-step scheme
3. Diagonally-implicit RK



- Preserves qualitatively the features of the original equation

Temporal discretization with FV Padé scheme

Illustration with implicit Euler scheme :

$$\mathcal{A}(\sigma^{(2)}, \theta) = \frac{1 + 2\alpha \cos \theta}{1 + 2\alpha \cos \theta + 4\gamma \sigma^{(2)} (\sin \frac{\theta}{2})^2}$$

- 2nd-order accurate in space : $\alpha = \frac{\gamma - 1}{2}$
- $\forall \gamma \neq 0, \partial_\theta \mathcal{A} < 0 \rightarrow$ non-oscillatory if $\mathcal{A}(\sigma^{(2)}, \pi) \geq 0$
- Two possibilities :
 - $\mathcal{A}(\sigma^{(2)}, \pi) = 0 \rightarrow \gamma = 2$
 - 2nd-order in time, 4th-order in space $\rightarrow \gamma = \frac{6}{5 - 6\sigma^{(2)}}$

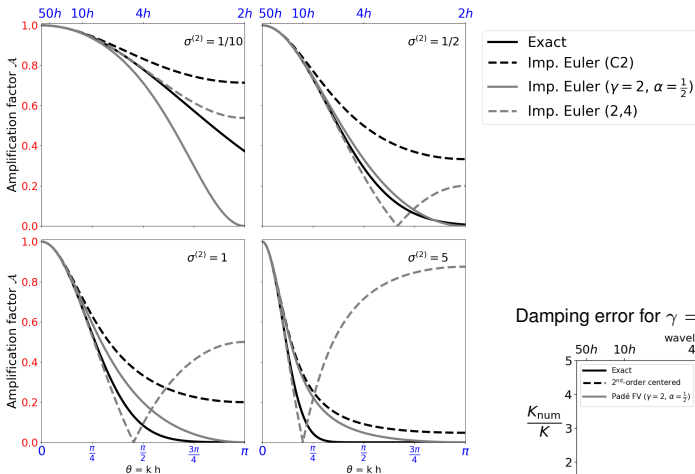
Implicit Euler + C2

$$\mathcal{A} = \frac{1}{1 + 4\sigma^{(2)} \sin(\theta/2)^2}$$

Implicit Euler + Padé FV ($\gamma = 2, \alpha = 1/2$)

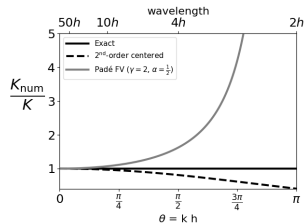
$$\mathcal{A} = \frac{1}{1 + 4\sigma^{(2)} \tan(\theta/2)^2}$$

Temporal discretization for diffusion



→ Padé FV scheme provides flexibility in the spatial discretization to counteract time discretization errors.

Damping error for $\gamma = 2$ and $\alpha = 1/2$



4

Combination with subgrid closure schemes

Mathematical stability of closure models (e.g. Deleersnijder et al., 2009)

- **An example** : analogy with a local Ri-dependent model

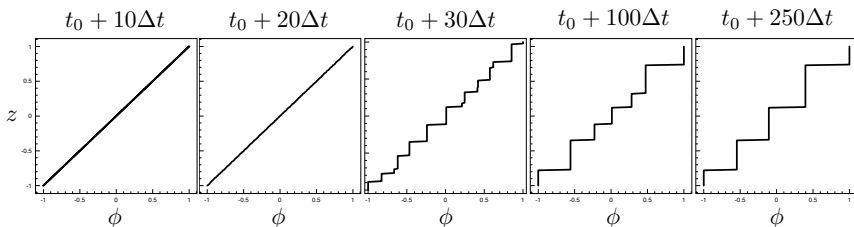
$$\partial_t \phi = \partial_z (K(z) \partial_z \phi), \quad K(z) = (\partial_z \phi)^{-2}$$

- ▷ $K(z) > 0 \rightarrow \phi$ remains bounded
- ▷ Original equation can be reexpressed as

$$\partial_t (\partial_z \phi) = \partial_z \left(\tilde{K}(z) \partial_z (\partial_z \phi) \right), \quad \tilde{K}(z) = -(\partial_z \phi)^{-2}$$

→ the gradient can grow unbounded

- **Numerical test** : $\phi(z, t = 0) = z$, $\phi(z = -1, t) = -1$, $\phi(z = 1, t) = 1$



Mathematical stability of closure models (e.g. Deleersnijder et al., 2009)

- **An example** : analogy with a local Ri-dependent model

$$\partial_t \phi = \partial_z (K(z) \partial_z \phi), \quad K(z) = (\partial_z \phi)^{-2}$$

- ▷ $K(z) > 0 \rightarrow \phi$ remains bounded
- ▷ Original equation can be reexpressed as

$$\partial_t (\partial_z \phi) = \partial_z \left(\tilde{K}(z) \partial_z (\partial_z \phi) \right), \quad \tilde{K}(z) = -(\partial_z \phi)^{-2}$$

→ the gradient can grow unbounded

- Ill-behaved solution due to the continuous formulation of the closure model and not to the details of its numerical discretisation
→ 0-equation closures are hard to study since it can change the diffusive nature of the equation
- More generally, spurious oscillations generally noticed are of a mathematical or a numerical nature ?

Energetic consistency – mixing terms vs turbulent closure

For X -equation closures with $X > 0$ a global energy budget can be derived

$$\begin{array}{rclcl} \partial_t u - \partial_z (K_m \partial_z u) & = & 0 & \rightarrow & \partial_t \text{KE} - \partial_z (K_m \partial_z \text{KE}) = -K_m (\partial_z u)^2 = -P \\ \partial_t b - \partial_z (K_s \partial_z b) & = & 0 & & \partial_t \text{PE} - \partial_z ((-z) K_s \partial_z b) = \frac{K_s}{z} \partial_z b = -B \end{array}$$

$$\partial_t \text{TKE} - \partial_z (K_e \partial_z \text{TKE}) = P + B - \varepsilon$$

Energy budget in a water column (ignoring the contribution of B.C.) :

$$E = \int_{z_{\text{bot}}}^{z_{\text{top}}} (\text{KE} + \text{PE} + \text{TKE}) dz \quad \rightarrow \quad \partial_t E = - \int_{z_{\text{bot}}}^{z_{\text{top}}} \varepsilon dz$$

- The discrete counterpart of it tells you exactly how to discretize forcing terms in the TKE equation

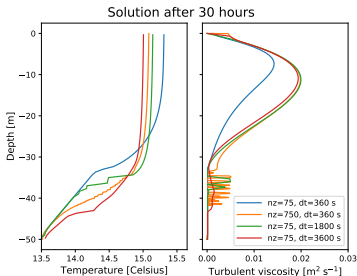
Wind-induced deepening of boundary layer

Kato & Phillips : *On the penetration of a turbulent layer into stratified fluid*, J. Fluid Mech., 1969

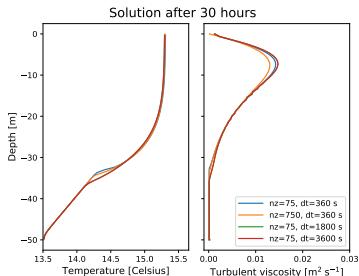
Price : *On the scaling of stress-driven entrainment experiments*, J. Fluid Mech., 1979

- ▶ Single column experiments with 0-equation closure (KPP, Large et al., 1994)
 - Use subgrid reconstruction to detect critical Ri-number
 - "Energy consistent" discretization of the Richardson number

Standard approach



Implicit Euler + FV Padé ($\alpha = 1/2$, $\gamma = 2$)



Summary

- Padé FV approach provides a good combination of simplicity and flexibility to handle diffusive terms with minimal changes in existing codes
 - Allows a good combination with surface layer param. and existing time-stepping
 - Provides degrees of freedom to mitigate numerical errors in time or to impose desired properties
- Simple single column test (Kato & Phillips) indicates a reduced sensitivity to numerical parameters

Perspectives

- Nonlinear stability (inputs on known pathological behaviors are welcome)
- Bottom boundary condition
 - Neutral case \rightarrow stratified case
- Single column tests & global ocean simulation within NEMO
- Add representation of oceanic molecular sublayer + MO layer in the top most oceanic grid box for OA coupling purposes (e.g. Zeng & Beljaars, 2005)